SCI INSTITUTE
TECHNICAL REPORT

Automatic Tissue Classification for the Human Head from Multispectral MRI

Tolga Tasdizen, David Weinstein, James N. Lee

UUSCI-2004-001

Scientific Computing and Imaging Institute
University of Utah
Salt Lake City, UT 84112 USA

March 5, 2004

Abstract:

A robust, automatic algorithm is presented for classifying multispectral MR scans of the human head into nine tissue classes. User initialization is not required. The proposed algorithm is based on three principles: (i) a combination of scalar and multispectral Expectation-Maximization clustering stages are used for fast, unsupervised statistical analysis, (ii) the minimal required amount of prior anatomical knowledge is used to solve statistical ambiguities, and (iii) a top-down modular approach that breaks the problem into smaller logical pieces is adopted.

THE U
UNIVERSITY
OF UTAH

Chapter 1

Introduction

Classification of head magnetic resonance imaging (MRI) data into distinct tissue classes is an important problem in biomedicine. Applications of MRI segmentation range from patient diagnosis to surgical planning to neurophysiology. We propose an automatic method for accurate and robust classification of the head into a set of nine tissue classes: gray matter (GM), white matter (WM), cerebrospinal fluid (CSF), blood vessels and sinuses, eyes, bone, bone marrow, muscle, and fat tissue.

The values recorded by an MRI scan are a function of tissue properties and the settings of the scanner. There is no single scan setting that can reliably discriminate between all of the tissues of interest; hence, we consider a method that makes use of a set of scans, *i.e.* multispectral data, each acquired with different settings. Even with multispectral data, a single step statistical classification of the entire head is an attractive but elusive goal as it is impossible to discriminate between certain tissues, such as white matter and fat, or bone marrow and muscle, based only on the histogram of MR data values. This observation suggests the use of prior knowledge to guide the classification process.

For a segmentation method to be useful in clinical applications, it should be fast, robust, and mostly automatic. To realize this goal we propose a modular, statistical approach that is supplemented with the minimum required amount of prior anatomical knowledge. Statistical methods have generally been successful for brain segmentation (see Chapter 2). We extend such methods to cover the entire head by dividing the problem into stages. For instance, we first do a brain/non-brain separation, followed by a bone/scalp separation for the non-brain region. These routines use statistics of the data as well as some basic anatomical knowledge of the head. This stage is followed by separate intra-region classifications based on the multispectral data. To speed up these multispectral classification routines, we initialize them with a pre-classification generated from a one-dimensional (scalar) subspace of the data. The software that implements this algorithm is freely available as part of the BioPSE [1] system, which can be downloaded at `http://software.sci.utah.edu/biopse.html`.

The rest of this report is organized as follows. Chapter 2 gives an overview of related work on MRI brain segmentation. In Chapter 3, we discuss statistical properties of multispectral MRI of the human head. Chapter 4 introduces the principles underlying our approach, and Chapter 5 gives

implementation details. Chapter 6 concludes with a discussion of experimental results.

Chapter 2

Background

In this chapter, we give a partial overview of the extensive literature on MRI segmentation. Researchers have proposed single scan brain segmentation methods that require varying degrees of user input [2] and fully automatic methods [3]. Fletcher *etal.* demonstrate that a single MRI can not discriminate between all tissue types of the human head [4]. In the same work, pure T1, T2 and proton density (PD) images are estimated from a sequence of 14 MR images, and supervised clustering techniques are used to classify six tissue classes. Other automatic multispectral methods use fuzzy clustering [5], Gibbs random fields [6], morphology [7], and non-parametric discriminant analysis [8].

MR images suffer from partial voluming, which occurs when multiple tissue types are present in a single voxel. Data statistics can significantly differ from Gaussian distributions due to this averaging effect. Laidlaw *etal.* use a Bayesian classification based on local histograms to handle partial voluming effects [9]. Another approach is to use Markov Random Field type models to ensure tissue continuity in the classification [6, 10, 11]. Active contour models, such as snakes, impose similar smoothness constraints and have also been used to segment regions of interest in brain MRI [12, 13]. Other model-based approaches deform a human brain atlas to match the data, or co-register the data to a spatial template of *a priori* probabilities for tissue types [14, 15].

Our approach targets to classify the entire head into a large number of tissue types because a complete model is required for many physical simulations (*e.g.* bioelectric field problems). It differs from deformable models and atlas-based approaches because we use only a minimal amount of low-level priors to augment our statistics. These priors are derived from basic observations such as "the skull encloses the brain in axial slices above the eyes" and "the probability of occurrence of muscle tissue is much larger below the eyes than above." We also propose a unique combination of 1D and multispectral classifiers that result in a fast and robust automatic classification method.

Chapter 3

Statistical Properties of Multispectral MRI

In this chapter, we investigate the statistical properties of multispectral MR datasets by examining their joint histograms. In this paper, we use multispectral MRI datasets that consist of T1, T2 and PD weighted images. Due to the difficulty in visualizing 3D histograms, Figure 3.1 illustrates a pair of 2D joint histograms. Figure 3.1(a) and (b) are the joint histograms for the PD-T1 and PD-T2 values in our data. These are histograms generated from human head MRI; hence, they represent the tissue types in the human head: white and gray matter, CSF, fat, muscle, bone, etc. Figure 3.1 shows the difficulties in classifying these tissue types based only on histogram methods.

The Brain Web database [16, 17] provides simulated MR scans of the human head with ground truth. Figure 3.2 shows the joint histogram of that data color coded with the tissue classes obtained from ground truth. The overlaps between the histograms of five classes can be seen more clearly. To illustrate the difficulties with pure statistical methods, we attempted classification with k-means clustering. The classification and ground truth of some of the tissue classes are shown in Figure 3.3. Notice that there is a lot of non-brain matter misclassified as various brain tissues. Especially a lot

(a)   (b)
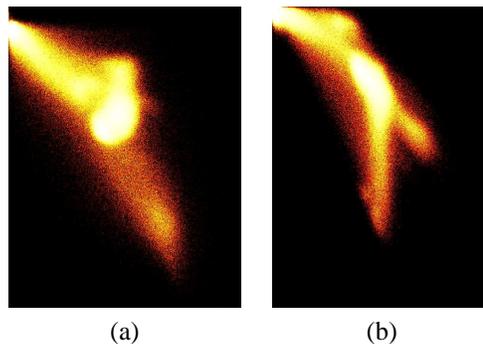
Figure 3.1: Multispectral MRI of the human head :(a) PD-T1 and (b) PD-T2 joint histograms.

of fatty tissue is classified as white matter.
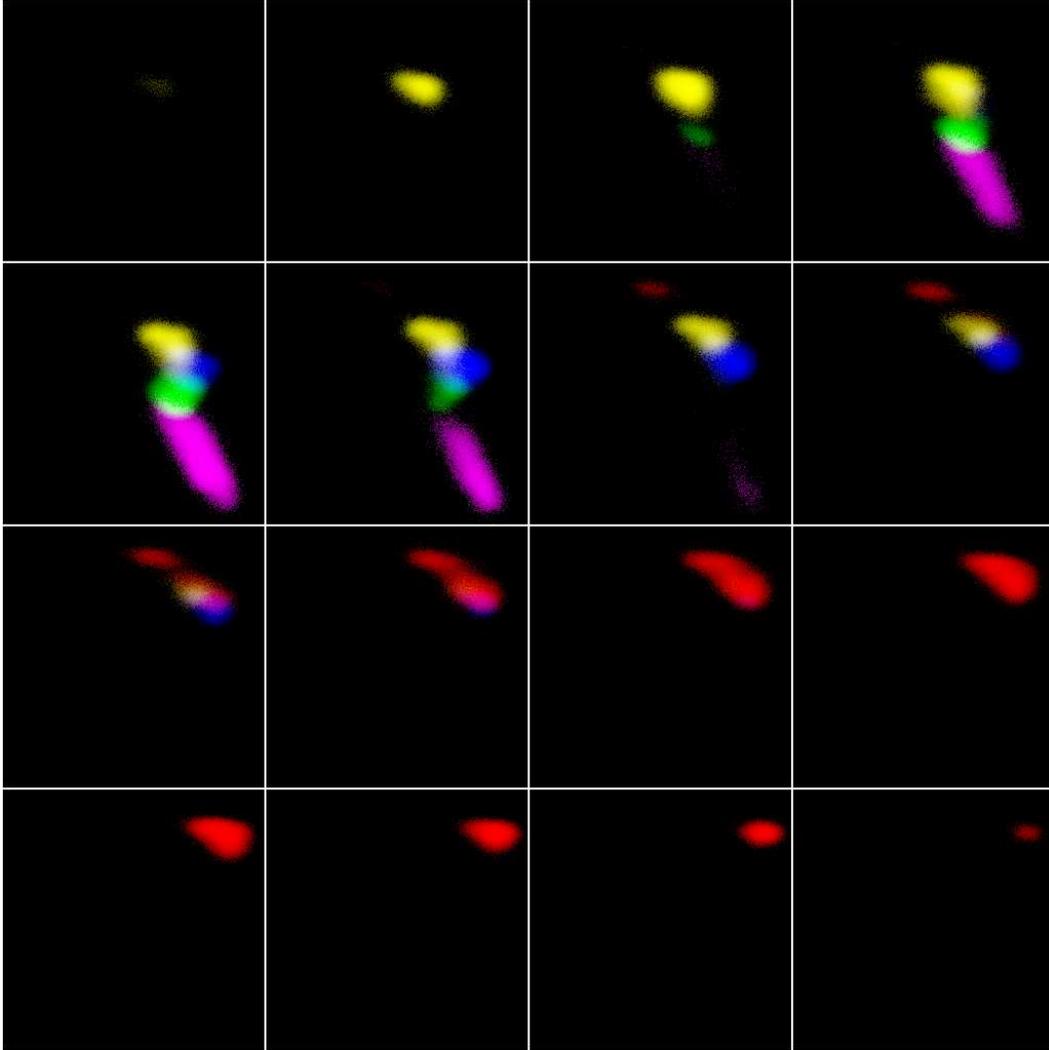
Figure 3.2: Horizontal axis T1, vertical axis PD, slices T2. CSF (red), white matter (green), gray matter (blue), muscle (yellow) and fat (magenta).

(a)

(b)

(c)

(d)

(e)

(f)
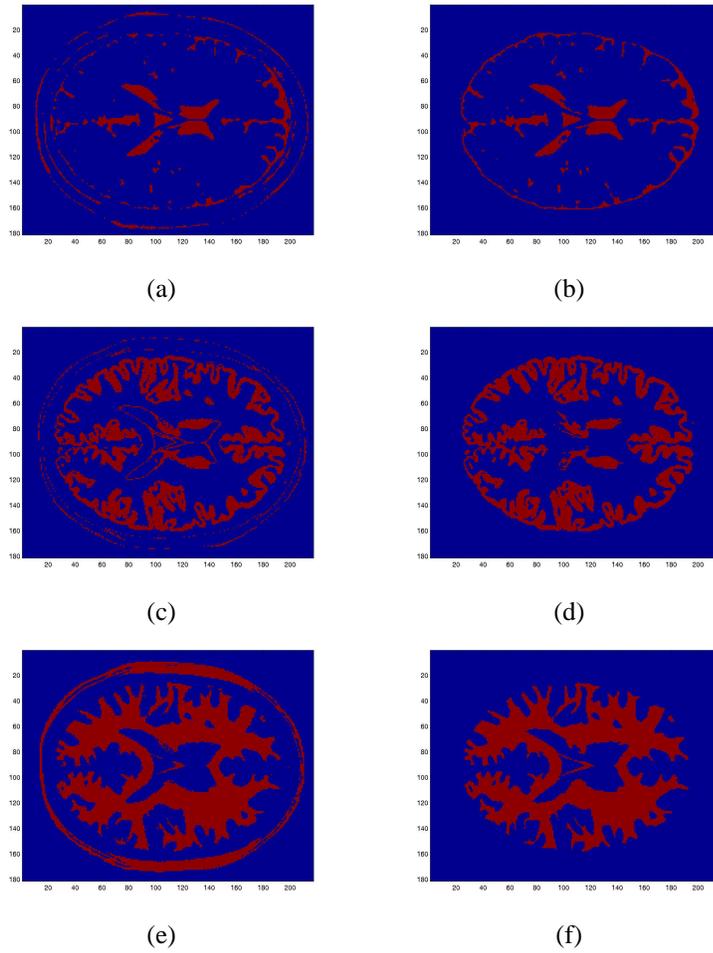
Figure 3.3: First column classification, second column ground truth. Rows from top to bottom: CSF, gray matter and white matter.

Chapter 4

Methods

Our multispectral data sets consist of T1, T2 and PD weighted axial scans and an optional T1-weighted "Fatsat" scan that are acquired in the same session. We will refer to these volumes as $T1^*$, $T2^*$, PD^*, and $T1^*_{fs}$. Figure 4.1 illustrates the flow chart of our algorithm. The remainder of this chapter discusses the underlying principles for each part of the algorithm; implementation details can be found in [18].

4.1   Background/Foreground Separation

The separation of background and foreground does not require the use of full multispectral MRI. It is possible to use just the $T1^*$ or PD^* scan; however, by defining an energy function as $E = T1^* + T2^* + PD^*$, we can achieve a better signal to noise ratio. The main statistical inference engine used in our system is the Expectation-Maximization (EM) algorithm. Here, it is used to learn the parameters (mean, variance and prior) for foreground and background classes from the global histogram of the energy function. For our foreground/background threshold, we choose the E value where the probabilities of the two classes are equal when evaluated based on the learned parameters. Because the background variance is much lower than the foreground, this value is always closer to the mean of the background distribution. Since the head is surrounded by a skin layer, which has large E values, using this threshold and flood filling from the boundaries of the volume, we can obtain a background/foreground separation. The results shown in Figure 4.2(b,e) are noisy; some of this is due to
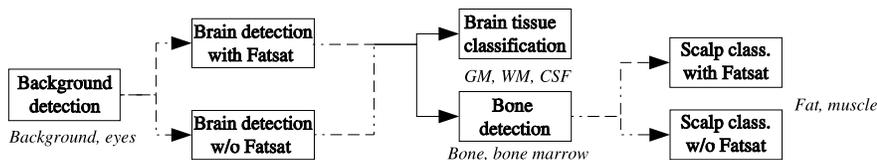
Figure 4.1: Tissue classification flow chart.

8
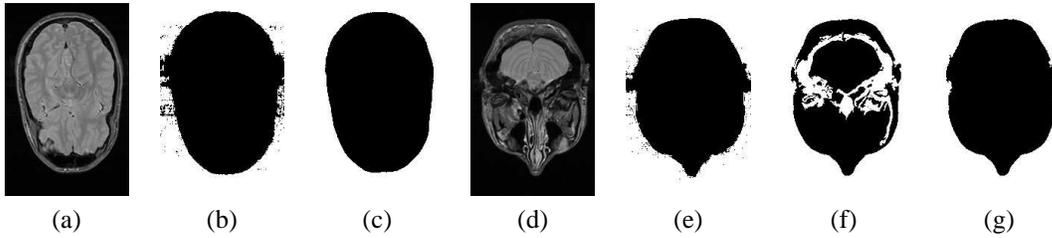
Figure 4.2: (a,d) Two slices of the energy volume, (b,e) low threshold, (c,f) high threshold, (g) morphology is used for slices below the eyes.

the partial voluming effect between the skin and the background. In such case, a higher threshold, which is the average of the means learned from the EM algorithm, would be more appropriate. The results shown in Figure 4.2(c,f) are good for slices at the top of the head, but for lower slices the background leaks into the bones and air cavities in the head through the ear canals due to this higher threshold.

To solve this problem, we divide the head volume into upper and lower using the location of the eyes. The eye tissue type exhibits very high $T2^*$ and low $T1^*$ values and is easily detected using a sphere detector of the appropriate size (25mm diameter) on the $T2^*$- $T1^*$ signal. Then, for slices above the eyes, morphological closing is performed before the flood fill to stop the leakage via the ear canals, see Figure 4.2(g).

4.2   Brain/Non-brain Tissue Separation

As in Section 4.1, full multispectral information is not needed for brain/non-brain separation, and we again use the energy function E. Figures 4.3(a) and (b) illustrate the histogram for E before and after the removal of the background voxels, respectively. In Figure 4.3(b), three distinct classes are present. These are, from lowest to highest mean value, bone, muscle and a combination of all brain tissues and fatty tissues in the scalp. We learn the distribution parameters of these classes using the EM algorithm on the histogram. We observe that bone has a higher mean value than the background. Without the removal of background voxels, it would be impossible to learn the correct parameters for the bone class because it would not be distinguishable from the background in the histogram.

We choose a threshold that separates the classes with the two highest means. For slices above the eyes, the skull encloses the brain, see Figure 4.3(c). Therefore, a flood fill from inside the brain using this threshold is enough to separate brain tissues from non-brain tissues, see Figure 4.3(d). However, in slices below the eyes the skull does not enclose the brain; the main problem is the orbital fat tissue around the eyes that comes into close proximity of the brain, see Figure 4.3(e). Fat has a high energy signal; hence, orbital fat around the eyes forms a bridge where the flood fill from within the brain can leak to other tissues.

A preliminary, threshold based fat detection is used to form an additional barrier against the flood fill in slices around the eyes where orbital fat occurs. If the optional T1 Fatsat volume that suppresses the signal from fatty tissues has been acquired, $T1^*$-$T1^*_{fs}$ provides a very good indicator of fat, and
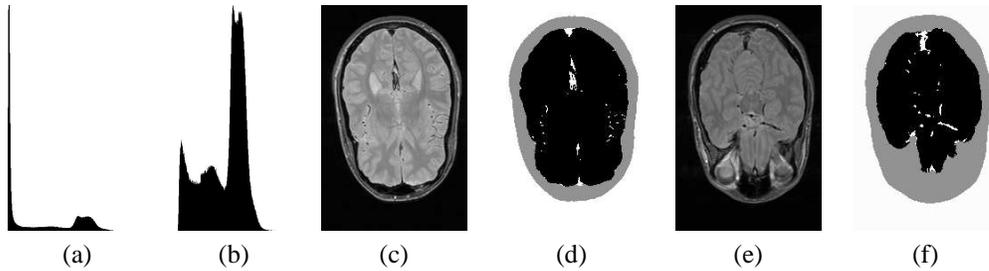
Figure 4.3: (a) Energy function histogram (a) before and (b) after removal of the background voxels. The scales of the y-axis are different. (c,e) two slices of the energy volume and (d,f) brain/non-brain tissue separation: black, gray and white voxels denote brain, non-brain and the sinuses.

the EM algorithm is used to learn fat and non-fat classes. Otherwise, the EM algorithm is applied only on the T1 scan using the observation that fat along with white matter has the highest T1 values. The white matter voxels are removed based on their higher distances from the background than fat voxels.

Blood vessels enclosed in the brain and sinuses between the brain and the skull have small E values because we apply a saturation pulse to blood below the acquisition slices. This pulse is necessary to avoid flow artifacts in the surrounding tissue. Therefore, sinuses and vessels are not included in the brain tissue voxels by the flood fill. Figures 4.3(c-f) illustrate results of the brain/non-brain separation and blood vessel detection: black, gray and white voxels denote brain, non-brain, and blood vessel types, respectively. Using the observation that the inside of the skull should have a smooth round shape, sinuses are detected using a morphological closing operation with a spatially adaptive mask that has a larger support in the direction along the brain boundary. The white voxels on the top periphery of the brain in Figures 4.3(d,f) are examples of detected sinuses. To detect blood vessels and sinuses inside the brain, we use morphological closing on the brain voxels with a small circular mask.

4.3   Brain Tissue Classification

An overview of the extensive research on segmentation of the brain MRI into GM, WM and CSF compartments was given in Section 2. While the multispectral EM algorithm is very suitable for the task, its convergence rate is very slow compared to scalar EM due to the much larger search space for parameters. Since the multispectral EM algorithm is the computational bottleneck in our approach, we can save significant computation time by providing an initialization from scalar data that is close to the final classification. An investigation of the one-dimensional subspaces of our multispectral data shows that the scalar signal $T2^*$- $T1^*$ provides good discrimination between GM/WM versus CSF and acceptable discrimination between GM versus WM. We will refer to this scalar signal as the *csf discriminant* because it takes on large positive values only at CSF voxels. For GM its value is close to 0, and for WM its value is negative. We compute the histogram of the *csf discriminant* for the brain tissue voxels and learn three Gaussian distributions from it. The results obtained from this scalar classification are shown in Figures 4.4(a) and (c). Notice that while CSF is classified reliably, there is some noise in the GM/WM classification.

10

<div align="center">(a)   (b)   (c)   (d)</div>
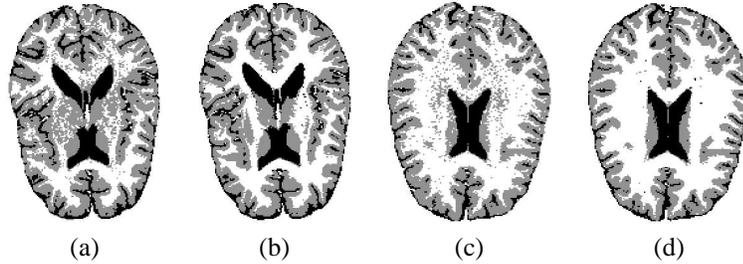
Figure 4.4: Brain tissue classification for two subjects: Initialization by scalar EM classification (a,c), and results of multispectral EM classification (b,d).

Using these results to initialize the multispectral EM algorithm, only a few iterations (25 for all examples in this report) are needed for convergence. Without a proper initialization, an order of magnitude more iterations are required. Figures 4.4(b) and (d) illustrate the results obtained with the multispectral EM. In this report, we do not address the bias field problem. In practice, we have not witnessed any significant bias-field effects. However, we note that existing methods, such as [19], can be incorporated into the EM classification routines.

4.4 Non-brain Tissue Classification

The non-brain tissues in our classification are bone, bone marrow, fat and muscle. The distribution of bone marrow values overlaps significantly with muscle in the multispectral domain; however, bone marrow occurs predominantly in the upper half of the head whereas muscle occurs predominantly in the lower half. Using this observation, we first separate bone tissues from the scalp tissues. Bone has very low (but non-zero) signal in all spectral dimensions, but the difference from other tissues is most pronounced in the PD^* scan. Therefore, we use the EM algorithm on the histogram of the PD^* volume for the non-brain tissues to learn two classes. Then we use an adaptive threshold to separate bone and bone marrow from the other tissues. This threshold is higher (closer to the mean of the scalp tissue class) for the top of the head, and lower (closer to the mean of the bone class) for the bottom half, reflecting our observation that bone marrow occurs predominantly above the eyes. Air cavities inside the head are classified as bone by the scheme described above. Air has the same characteristics as the background outside the head, whereas bone has low but non-zero mean in all channels. We compute the standard deviation of the background voxels and use this as a threshold for identifying air voxels; outliers are removed by morphological opening and closing operations. The final step is to classify the scalp into fat and muscle tissues. To initialize the multispectral EM algorithm, we use the threshold that was computed for fat tissues in the brain/non-brain separation step. We use the full multispectral information, including the $T1^*_{fs}$ volume if available, for the final classification between fat and muscle.

Chapter 5

Implementation

In this chapter, we discuss the various stages of the algorithm in more detail. Throughout the progress of the algorithm, voxel classifications are stored in a volume which we call Labels. This volume is initialized as unclassified and as the various stages of the algorithm are run, labels are assigned to voxels. We use final and temporary labels. Background, GM, WM, CSF, fat, muscle etc. are examples of the former, whereas, foreground, brain and non-brain are examples of the latter. As a principle, all stages of the algorithm operate on voxels with temporary labels. In other words, once a final label is attached to a voxel it is no longer used in the rest of the stages.

5.1   Eye Detection

The eye tissue type exhibits very high $T2^*$ and low $T1^*$ values, which is unambiguously separated from surrounding tissue, and has roughly a spherical shape with approximate diameter 25 millimeters. Using these observations, we can robustly detect the location of the eyes by convolving the $T2^*$- $T1^*$signal with a spherical mask of diameter 25mm and looking for the maximum response locations. However, 3D convolution is a computationally expensive task. We can speed up this search if we restrict the search space to a subset of the volume by fist doing a 2D search.

Step 1 - 2D search

```
Assumption: The head is roughly centered in the axial slices. The
face is pointing towards higher y-values.

Define xl = 0.25*width, xm = 0.5*width, xh = 0.75*width
Define yl = 0.66*height

For every z-slice, do
   Convolve the image subregions [x=xl:xm,y=yl:height] and
   [x=xm:xh,y=yl:height] with a circular binary mask of radius
```

```
12.5 mm.
Find the maximum response and its location in each subregion
```

```
Find the z-slice with the maximum response, call it z'. Define the
centers of the two eyes as the location of that maximum responses
in the z' slice.
```

Step 2 - 3D search and flood fill

```
Do 3D convolution in volume subregions within 10mm of the eye
centers with a sperical mask of radius 12.5mm.
```

```
Find the maximum response for both subregions. Redefine the eye
locations to be at these 3D maximal response points.
```

```
Define a threshold as 0.75 times the maximal response over the
volume of the spherical mask. Flood fill from the two eye center
locations upto this threshold to identify eye voxels, mark these
voxels in the Labels volume.
```

5.2   Background/Foreground Separation

We define an energy function as the sum of different MR scans $E = T1^* + T2^* + PD^*$. The global histogram for this energy function consists of a peaked distribution at small values (background) and a broad distribution at larger values (foreground).

Step 1 - Expectation Maximization

```
Build a global histogram of the energy function excluding the
already detected eye voxels. Build a cumulative distribution
function (cdf) from the normalized histogram. The cdf has
value 0 for the lowest E value and monotonically increases until
it reaches 1 for the highest E value.
```

```
Initialize the parameters of the foreground and background classes
as follows:
Background mean = 0
Foreground mean = E value where cdf is 0.5
Standard deviation foreground = (foreground mean - bg. mean)/4
Standard deviation background = foreground standard deviation/4
Both priors = 0.5
```

```
Run the EM algorithm until convergence or the maximum number of
iterations is reached. Convergence is reached if the change in
means per iteration divided by the respective standard deviations
```

```
drops below a preset threshold (0.001) in our case. Maximum
number of iterations is 1000. The same convergence criteria are
used in all EM stages unless otherwise noted.

Define low threshold, th_low = E value where probabilities of
the 2 learned classes are equal.
Define high threshold, th_high = average of the 2 means learned
from EM.
```

We can not simply classify the volume into foreground/background based on thresholding because such an approach would mislabel the bone and parts of bone marrow tissues as background. Since the head is surrounded by a skin layer, which has large E values, using this threshold and flood filling from the boundaries of the volume, we can obtain a background/foreground separation. For lower slices below the eyes, the background leaks into the bones and air cavities in the head through the ear canals. Therefore, we have to treat the volume in two parts.

Step 2 – Flood fill

```
For z-slices above the center of the eyes (the top of the head), do
   2D slice floodfill from the image boundaries using th_high to
   determine background voxels.
   Compute an image of 2D distances to the closest background
   pixel.

For the rest of the z-slices, do
   Create an image with values 1 if E>th_high, 2 if E>th_low,
   0 otherwise.
   If a pixel is marked as 2, and the distance of that pixel
   in the z-slice before the current is greater than 10mm
   (at least 10mm inside the head), do a floodfill from this pixel
   that marks as 1, pixels marked as 2.
   Mark as 0, the remaining pixels marked as 2.
   Do a floodfill from the image boundaries to find pixels marked
   as 0 that are connected to the image boundaries, mark these
   pixels as background.
   Mark the rest of the pixels as foreground.
   Compute an image of 2D distances to the closest background
   pixel.
```

5.3   Preliminary Fat Detection

To separate the brain tissues from non-brain tissues we can threshold the energy function and use a flood fill. This is based on the observation that brain tissue appears brighter than other tissues with the exception of fat and for slices above the eyes, the skull encloses the brain and a flood fill from inside the brain using a threshold is enough to separate brain tissues from non-brain tissues.

However, in slices below the eyes the skull does not enclose the brain; the main problem is the orbital fat tissue around the eyes that comes into close proximity of the brain. So the next step is to do fat detection in these slices before the floodfill operation to detect the brain.

Fat detection is easy if the FatSat scan has been acquired:

Preliminary Fat Detection with the FatSat scan

```
Define the fat discriminant signal as F = T1 - T1fatsat.

Build a histogram of this function for the foreground voxels.
Build a cumulative distribution function (cdf) from the normalized
histogram.

Initialize a 2-class EM algorithm as follows:
Non-fat class mean    = value of F where cdf is 0.4
Fat class mean        = value of F where cdf is 0.9
Non-fat class prior   = 0.8
Fat class prior       = 0.2
Non-fat class s. dev = Difference in means/10
Fat class s. dev      = same as above


Run the EM algorithm until convergence or the maximum number
of iterations is reached.

Define a threshold, th_fat = F value where probabilities of
the fat and non-fat classes match. Mark pixels in z-slices
below z = Top level of eyes - 6mm that are above th_fat with
a temporary fat label.
```

If the FatSat scan has not been acquired, we have to perform a more complicated 4-class EM stage followed by morphology to remove unwanted voxels.

Preliminary Fat Detection with the FatSat scan

```
Define the fat discriminant signal as the T1 signal.

Build a histogram of this function for the foreground voxels.
Build a cumulative distribution function (cdf) from the normalized
histogram.

Initialize a 4-class EM algorithm as follows:
Non-fat class1 mean    = T1 value where cdf is 0.1
Non-fat class2 mean    = T1 value where cdf is 0.3
Non-fat class3 mean    = T1 value where cdf is 0.6
Fat class mean         = T1 value where cdf is 0.9
Non-fat class1 prior   = 0.2
Non-fat class2 prior   = 0.2
```

```
Non-fat class3 prior   = 0.4
Fat class prior        = 0.2
All s. dev.s = (Non-Fat class2 mean - Non-fat class1 mean)/10
Run the EM algorithm until convergence or the maximum number
of iterations is reached.

Define a threshold, th_fat = F value where probabilities of the fat
class and the non-fat class3 match.

Mark pixels in z-slices below z = Top level of eyes - 6mm that
are above th_fat with a temporary fat label. Then for all of
these z-slices do a morphological closing, opening and dilation
with a circular mask of radius 4 voxels. These series of
operations remove isolated white matter pixels marked as fat
and extend the boundaries of other temporary fat areas.
```

5.4   Brain/Non-brain Tissue Separation

The same energy function E defined for background/foreground separation, is also used for Brain/non-brain tissue separation. After removal of the background voxels, a histogram of the E function for the remaining voxels shows three distinct classes. These are, from lowest to highest mean value, bone, muscle and a combination of all brain tissues and fatty tissues in the scalp. The first step is to use the EM algorithm to learn the parameters for these classes.

Step 1 - Expectation Maximization

```
Build a histogram of the energy function for the foreground
voxels.
Build a cumulative distribution function (cdf) from the
normalized histogram.

Initialize the parameters of the 3 classes as follows:
Bone class mean        = 0
Muscle class mean      = E value where cdf is 0.2
Brain/fat class mean   = E value where cdf is 0.65
Bone class prior       = 0.1
Muscle class prior     = 0.2
Brain/fat class prior  = 0.7
Bone class s. dev.     = Muscle mean / 10
Muscle class s. dev.   = 9*Bone class s.dev
Brain/fat class s. dev. = 6*Bone class s.dev

Run the EM algorithm until convergence or the maximum
number of iterations is reached.

Define a threshold, th_brain = E value where probabilities
```

of the brain/fat and muscle classes match.

The next step is to use th_fat from **Step1** and the fat voxels from the previous section in conjunction with a flood fill to extract the brain voxels.

Step 2 - Flood fill and morphology

```
For z-slices from the top of the head to the eyes, do
  For all foreground pixels, if E>th_brain mark pixel as 1,
  otherwise as 0.
  Exception: For slices within 9 mm of the eyes, all pixels
  with y greater than the center position of the eyes and with
  a distance less than 15 mm from the background are always
  marked as 0.
  Floodfill from slice center to find a connected component
  of 1's.

For z-slices from the eyes and below, do
  For all foreground pixels, if E>th_brain mark pixel as 1,
  otherwise as 0.
  Exception: For slices within 9 mm of the eyes, all pixels
  with y greater than the center position of the eyes are
  always marked as 0.
  Morphological opening to remove small connections between
  disconnected regions of pixels marked as 1.

Do a 3D flood fill from the center of the slice at the level of
the eyes (limited only to z-slices from the eyes and below), to
find a connected component of 1's.

For all z-slices, do
  Morphological closing with a circular mask of radius 4 pixels
  to close any small holes in the brain matter. This will
  generally include all blood vessels in the brain which appear
  dark.
  Morphological closing with a mask that has 10mm support in the
  direction tangential to the distance from the background, but
  only 1.5 mm wide in the perpendicular direction. This closing
  will find sinuses that are sandwiched between the brain and
  the skull that appear as wedges missing from the brain.

For all voxels marked as brain, mark all with E<th_brain as
sinuses. Umark all temporary fat pixels.
```

5.5 Brain Tissue Classification

The scalar signal $T2^{*}$-$T1^{*}$ provides good discrimination between GM/WM versus CSF and acceptable discrimination between GM versus WM. We will refer to this scalar signal as the *csf discriminant* because it takes on large positive values only at CSF voxels. For GM its value is close to 0, and for WM its value is negative. We first compute the histogram of the *csf discriminant* for the brain tissue voxels and learn three Gaussian distributions from it.

```
Define the csf discriminant, C,  signal as the T2-T1 signal.

Build a histogram of this function for brain voxels.
Build a cumulative distribution function (cdf) from the normalized
histogram.

Initialize a 3 class EM algorithm as follows:
White matter class mean    = value of C where cdf is 0.2
Gray matter class mean     = value of C where cdf is 0.65
CSF class mean             = value of C where cdf is 0.95
White matter class prior   = 0.45
Gray matter class prior    = 0.45
CSF class prior            = 0.1
White matter class s. dev = diff. in white/gray matter means/4
Gray matter class s. dev  = diff. in white/gray matter means
CSF class s. dev           = same as above

Run the EM algorithm until convergence or the maximum number of
iterations is reached. This stage uses the T1, T2 and PD scans, it
doesn't use the Fatsat scan.

Using the probability function obtained from the scalar EM compute
multispectral means and variances for the 3 classes.

Run the multispectral EM algorithm for 25 steps. (Due to its
computational complexity we run this stage only for a fixed
number of iterations; however, because of the good initialization
provided by the scalar EM, this number is enough for getting very
close to convergence.)

Using the resulting probability functions, mark each brain voxel
as WM, GM or CSF.
```

5.6 Bone detection

Bone has very low (but non-zero) signal in all spectral dimensions, but the difference from other tissues is most pronounced in the PD^{*} scan. Therefore, we use the EM algorithm on the histogram

of the PD^* volume for the non-brain tissues to learn two classes.

Step 1 - Expectation Maximization

```
Build a histogram of the PD scan for the remaining foreground
voxels.
Build a cumulative distribution function (cdf) from the
normalized histogram.

Initialize a 2-class EM algorithm as follows:
Bone/air class mean    = PD value where cdf is 0.15
Scalp class mean       = PD value where cdf is 0.65
Bone/air class prior  = 0.3
Scalp class prior      = 0.7
Bone/air class s. dev = Bone/air class mean
Scalp class s. dev     = 2 times Bone/air class s.dev

Run the EM algorithm until convergence or the maximum number
of iterations is reached.
```

Step 2 - Morphology

```
Define th_low  = average of bone/air and scalp class means
Define th_high = (bone/air class mean + 2 x scalp class mean)/3

For z-slices from the top of the head to 15mm above the eyes, do
  Define a threshold,
    if z more than 35mm above the eyes th = th_high
    else th varies linearly to have the values th_high and
    th_low at 35mm and 15mm above the eyes, respectively.

  Threshold the PD signal with th.

  Morphological closing with a mask that has 10mm support in the
  direction tangential to the distance from the background, but
  only 2 mm wide in the perpendicular direction. This will close
  holes in the bone.

  Flood fill from non-bone pixels touching the background. Mark
  these pixels as scalp. The rest of the pixels are marked as bone
  if their PD<th, as marrow otherwise.

For the rest of the z-slice, simply threshold with th_low.
```

Air cavities inside the head are classified as bone by the scheme described above. Air voxels are removed with the following procedure.

19

Step 3 - Air cavity removal

```
Compute the standard deviation of background voxels, call
this value s.

Mark voxels with E<s/2. Morphological opening with a circular
mask of radius 2 voxels. Flood fill from remaining locations
using the threshold s. Mark these as air voxels.
```

5.7   Scalp Classification

The remaining tissue types are fat and muscle. We initialize this classification using results from the preliminary fat detection stage.

```
Using the threshold computed for fat in preliminary fat detection,
mark remaining voxels as fat or muscle. Compute initial
multispectral mean, variance and prior quantities from this
classification.

Run a multispectral EM stage for 25 iterations. This stage uses
all available scans, including T1Fatsat if present.

Using the resulting probability function classify voxels as fat
or muscle.
```

Chapter 6

Results and Discussion

Figure 6.1 illustrates results of the classification algorithm on four slices from three subjects. The following scans were used: (i) t1-weighted spin echo (TE=15ms, TR=628ms), and (ii) t2-weighted and pd-weighted fast spin echo (TE1=15ms, TE2=105ms, TR=3000ms). Both scans use 2mm slices, 192x256 matrix with a 18x24cm field of view and presat pulse was applied inferior to slices to saturate inflowing blood. Total scan time was 33 minutes for 70 slices. Total computation time for the same volume was 16 minutes on an *Intel Xeon* 1.7 Ghz processor.

In Figure 6.1, the top and bottom rows show non-brain tissue classification, and the brain tissues and sinuses for the same slices, respectively. The classification in column 1/row 1 demonstrates several tissue types: the eyes, orbital fat around the eyes, the skull and the temporalis muscle on either side of the head as well as some muscle in the forehead between the eyes. In the second row, observe that the superior sagittal sinus has been detected at the top, as well as cerebral arteries below the center of the brain. Some noise is present in the classification between white and gray matter. As part of our future work, spatial continuity constraints will be introduced into the multispectral EM classifier using Markov Random Fields [6, 10, 11]. The classification in column 2/row 1 shows that air pockets inside the frontal bone of the skull, *i.e.* the frontal sinuses, have been successfully separated from the bone. The classification in column 4/row 1 illustrates the separation between bone and bone marrow.

We introduced an automatic method for classifying the human head into nine tissue compartments using T1, T2 and PD weighted MR scans. A potential application for the proposed classification is the construction of patient-specific, detailed conductivity models of the head for use in the inverse EEG problem. We also plan to perform a formal study of the proposed method using data with ground truth.

Figure 6.1: Top row: Bone (magenta), marrow (gray), fat (black), muscle (brown), eyes (gray), air (green). 2nd row: CSF (magenta), WM (gray), GM (black), sinuses (brown).

Bibliography

[1] BioPSE: Problem Solving Environment for modeling, simulation, and visualization of bioelectric fields. Scientific Computing and Imaging Institute (SCI), http://software.sci.utah.edu/biopse.html, 2002.

[2] J. C. Rajapakse, J. N. Giedd, C. DeCarli, J. W. Snell, A. McLaughlin, Y. C. Vauss, A. L. Krain, S. Hamburger, and J. L. Rapoport, "A technique for single-channel mr brain tissue segmentation: Application to a pediatric sample," *Magnetic Resonance Imaging*, vol. 14, pp. 1053–1065, 1996.

[3] N. Kovacevic, N. J. Lobaugh, M. J. Bronskill, B. Levine, A. Feinstein, and S. E. Black, "A robust method for extraction and automatic segmentation of brain images," *NeuroImage*, vol. 17, pp. 1087–1100, 2002.

[4] L. Fletcher, J. Barsotti, and J. Hornak, "A multispectral analysis of brain tissues," *Magnetic Resonance in Medicine*, vol. 29, pp. 623–630, 1993.

[5] D. L. Pham, J. L. Prince, A. P. Dagher, and C. Xu, "An automated technique for statistical characterization of brain tissues in magnetic resonance imaging," *I. J. of Pattern Recog. and Artificial Intelligence*, vol. 11, no. 8, pp. 1189–1211, 1997.

[6] C. Pachai, Y. M. Zhu, C. R. G. Guttmann, R. Kikinis, F. A. Jolesz, G. Gimenez, J.-C. Froment, C. Confavreux, and S. K. Warfield, "Unsupervised and adaptive segmentation of multispectral 3d magnetic resonance images of human brain: a generic approach," in *Proceedings of MICCAI*, pp. 1067–1074, 2001.

[7] H. G. Schnack, H. E. H. Pol, W. F. Baare, W. G. Staal, M. A. Viergever, and R. S. Kahn, "Automated separation of gray and white matter from mr images of the human head," *NeuroImage*, vol. 13, pp. 230–237, 2001.

[8] U. Amato, M. Larobina, A. Antoniadis, and B. Alfano, "Segmentation of magnetic resonance brain images through discriminant analysis," *J. Neuroscience Methods*, vol. 131, pp. 65–74, December 2003.

[9] D. H. Laidlaw, K. W. Fleischer, and A. H. Barr, "Partial-volume Bayesian classification of material mixtures in MR volume data using voxel histograms," *IEEE Trans. Medical Imaging*, vol. 17, no. 1, pp. 74–86, 1998.

[10] T. Kapur, W. E. L. Grimson, W. M. Wells, and R. Kikinis, "Segmentation of brain tissue from magentic resonance images," *Med. Im. An.*, vol. 1, pp. 109–127, 1996.

[11] K. Held, E. R. Kops, B. J. Krause, W. M. Wells, R. Kikinis, and H.-W. Muller-Gartner, "Markov random field segmentation of brain mr images," *IEEE Trans. Medical Imaging*, vol. 16, no. 6, pp. 878–886, 1997.

[12] A. Kelemen and G. G. G. Szekely, "Three-dimensional model-based segmentation of brain mri," in *Proc. IEEE Workshop Biomedical Image Analysis*, pp. 4–13, 1998.

[13] M. Atkins and B. Mackiewich, "Fully automatic segmentation of the brain in mri," *IEEE Trans. Medical Imaging*, vol. 17, pp. 98–107, 1998.

[14] J. Ashburner and K. J. Friston, "Multimodal image coregistration and partitioning – a unified framework," *NeuroImage*, vol. 6, pp. 209–217, 1997.

[15] J. Marroquin, B. Vemuri, S. Botello, F. Calderon, and A. Fernandez-Bouzas, "An accurate and efficient bayesian method for automatic segmentation of brain mri," *IEEE Trans. Medical Imaging*, August 2002.

[16] C. Cocosco, V. Kollokian, R.-S. Kwan, and A. Evans, "Brainweb: Online interface to a 3d mri simulated brain database," in *Proceedings of 3-rd International Conference on Functional Mapping of the Human Brain*, 1997.

[17] "http://www.bic.mni.mcgill.ca/brainweb/."

[18] T. Tasdizen, D. Weinstein, and J. N. Lee, "Automatic tissue classification for the human head from multispectral mri," Tech. Rep. UUSCI-2004-001, U. of Utah.

[19] W. M. Wells, W. E. L. Grimson, R. Kikinis, and F. A. Jolesz, "Adaptive segmentation of mri data," *IEEE T. Med. Imaging*, vol. 15, no. 4, pp. 429–441, 1996.